

REPRINTED FROM:

# OPTICS COMMUNICATIONS

Volume 40, No. 4, 15 January 1982

## HIGH REPETITION RATE EFFECTS IN XeCl TEA LASERS

R. BUFFA, P. BURLAMACCHI, M. MATERA \*, H.F. RANEA SANDOVAL \*\* and  
R. SALIMBENI

*Istituto di Elettronica Quantistica del C.N.R., Firenze, Italy*

pp. 288–293



NORTH-HOLLAND PUBLISHING COMPANY-AMSTERDAM

## HIGH REPETITION RATE EFFECTS IN XeCl TEA LASERS

R. BUFFA, P. BURLAMACCHI, M. MATERA \*, H.F. RANEA SANDOVAL \*\* and R. SALIMBENI

*Istituto di Elettronica Quantistica del C.N.R., Firenze, Italy*

Received 18 October 1981

The high repetition rate capability of a discharge pumped XeCl laser with static fill has been studied by double pulse experiments. By suitably selecting the laser parameters (energy deposition, gas mixture composition, filling pressure), following an analytical model of the discharge induced thermal effects, laser action from the second pulse for delays as short as 5 ns with an energy of 12.5 mJ has been achieved.

### 1. Introduction

The development of discharge pumped rare-gas halide (RGH) lasers has led in the past few years to the achievement of single pulse energies and gas mixture fill lifetimes which make them suitable for most experiments requiring UV coherent radiation. Intensive research has also been devoted to the high pulse repetition rate (PRR) operation of these lasers since, for many applications, especially in photochemistry, large average output powers with high overall efficiencies are required.

The most effective way to achieve high PRR operation in RGH lasers is to "clean" the discharge region by circulating the gas through the electrodes at high speed. At present, average output powers from 10 W to 200 W have been obtained by several researchers from transverse flow RGH lasers, with closed cycle or blowdown configurations [1-7]. The operating characteristics of these systems have shown that more than 5 gas replacements in the discharge volume between pulses are required to maintain the maximum energy per pulse.

However the great complexity of transverse gas flowing systems with high velocity is justified only for sufficiently high average powers. Since for certain applications, for example to injection lock a high energy device, high PRR lasers with high beam quality but relatively low average powers are required [8], some effort has also gone into the understanding and development of high PRR lasers at low [9] or medium [10] power levels without rapid gas flow. These experiments, investigating the relative weight of thermal and kinetic effects, have demonstrated the feasibility of high PRR operation by merely providing an effective cooling of the gas by heat transfer to the cell walls. To this purpose, an appropriate configuration is the waveguide cell, possibly with external electrodes, as in the case of capacitively coupled discharge [11] or microwave excitation [12].

Moreover, the relation between discharge stability and high PRR capability of RGH lasers has been demonstrated in a paper describing a 200 Hz resistively stabilized XeCl laser without gas circulation [13].

This paper describes an experimental investigation of the effects limiting the PRR in a discharge pumped XeCl laser with static fill. The dependence of the high PRR capability of this device on various parameters (energy deposition, discharge width, gas mixture composition) has been studied by double pulse experiments, showing an optimum working point for high PRR operation very far from that for maximum single pulse energy.

\* CNEN, Divisione Nuove Attività, Frascati, Italy.

\*\* Fellow of the Consejo Nacional de Investigaciones Científicas y Técnicas, República Argentina.  
Present address: Centro de Investigaciones Ópticas, La Plata, Argentina.

The results of this investigation, besides improving our understanding of the problems associated with the high PRR operation of a RGH laser, may lead to an optimization of: a) gas flowing systems, reducing to a minimum – possibly less than one – the number of required gas changes per pulse; b) static fill lasers, by using the most suitable energy deposition or heat dissipation configuration.

## 2. Double pulse experiments

In addition to the problems related to component reliability (optical windows transmission, thyatron recovery) and to gas contamination, the high PRR operation of discharge pumped RGH lasers presents problems arising from: a) thermal effects, causing density gradients which can destroy the discharge stability and the optical quality of the medium; b) formation of atomic or molecular species adversely affecting the excimer kinetics; c) breakdown voltage drop, leading to a reduction in energy deposition and consequently in pumping intensity.

In order to estimate the relative importance of the different effects for a XeCl laser, avoiding the masking due to the cumulative laser degradation related to the high average power, we have undertaken double pulse experiments. The following parameters were monitored: a) laser output, b) current pulse, c) breakdown voltage, d) 308 nm side-light fluorescence and e) transmission of a HeNe laser beam through the active medium after the discharge.

The laser used for this study was a conventional UV preionized type, designed for low PRR operation. The uniform-field profiled aluminum electrodes separated by 2 cm with a length of 90 cm were hand sanded to reduce intensified discharge regions. The pulse forming circuit, schematically shown in fig. 1, was of the charge transfer type, switched by a spark-gap. The discharge was stabilized by a sliding-arc preionization flashboard, driven by two 0.5 nF capacitors directly connected to the spark-gap. The optical resonator consisted of a dielectric coated high reflectivity ( $R \approx 98\%$ ) concave mirror of 10 m radius of curvature and an uncoated quartz flat, external to the cell sealed by two slightly misaligned quartz windows. The capacitor banks  $C_1$  and  $C_2$  were made of arrays of ceramic capacitors (Steatite and Porcelain Products Ltd., type C725) of 2.5 nF nominal capacitance each.

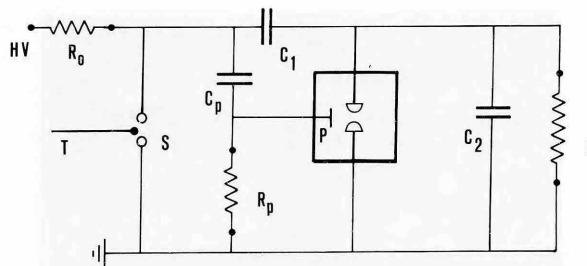


Fig. 1. Diagram of the laser charging circuit: T trigger, S spark-gap, P preionizer.

The configuration giving the maximum pulse energy ( $E \approx 100$  mJ), with a gas mixture containing 4 mbar HCl, 50 mbar Xe in He at a filling pressure of 2 bar, was  $C_1 = 80$  nF and  $C_2 = 50$  nF at a charging voltage of 30 kV. The  $C_1$  charging time constant was 2.5 ms.

Exciting the laser in this configuration with a double pulse we have observed for the normalized lasing energy of the second pulse  $E_2/E_1$  versus pulse separation  $T$  the behaviour reported in fig. 2.

The HeNe transmission experiment was conducted by enlarging the probe laser before passing it along the laser axis, in order to illuminate the discharge region with a uniform intensity over the cross section. A pin-hole of 1 mm radius was used to select the point of maximum disturbance, approximately in the center of the discharge. The detected signal for the maximum pulse energy configuration in a mixture containing 50 mbar Xe in He up to 2 bar is shown in fig. 3. The

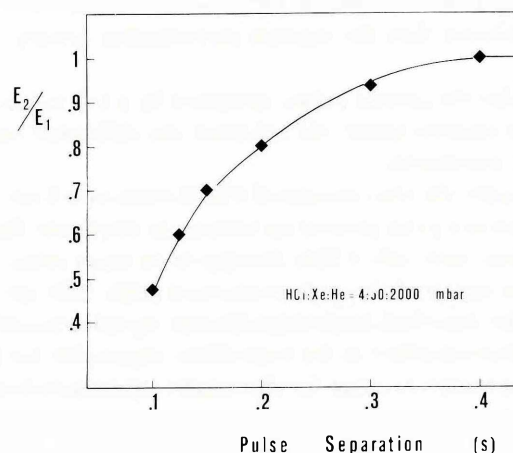


Fig. 2. Normalized energy of the second laser pulse versus pulse separation in the configuration of maximum pulse energy:  $C_1 = 80$  nF,  $C_2 = 50$  nF, HV = 30 kV.

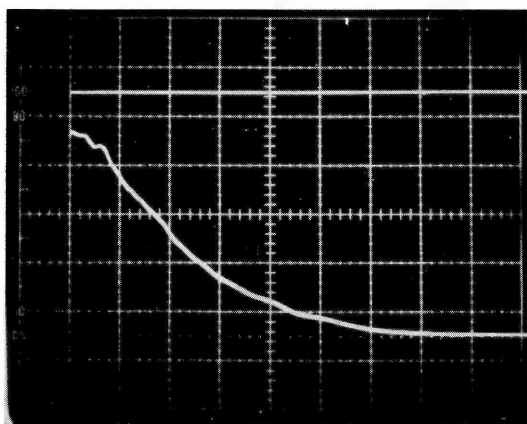


Fig. 3. Time evolution of the HeNe laser beam transmission through the discharge region (50 ms/div).

disturbance is seen to die out 300 ms after the discharge, denoting a strong thermal (optical) effect.

The voltage pulse across the electrodes was monitored by using a Tek P6015 high voltage probe. The detected waveforms for two pulses separated by 100 ms resulted as being completely superimposed. This result is consistent with the main atomic and molecular excited species lifetimes [14,15] and with the lifetime of the ionized species ( $\text{Xe}^+$ ,  $\text{Xe}_2^+$ ,  $\text{Cl}^-$ ). In fact the ionic density, following after the discharge the two body recombination law

$$n(t) = n(0)/(1 + kn(0)t),$$

with a rate constant  $k \sim 10^{-6} \text{ cm}^3 \text{ s}^{-1}$  [14], decays within 1 ms to a value of  $10^9 \text{ ions cm}^{-3}$ , which is quite lower than the estimate preionization density [16].

Also the current pulses, measured by a low inductance resistive probe, did not show any difference on their waveforms.

Lastly the time integrated side fluorescence from the second pulse showed an increase in amplitude fluctuation, with only a light decrease in its mean value, in the region of abrupt laser decrease (100–200 ms).

The described diagnostics allowed the selection of the thermal effect as the main effect responsible for the lasing energy decrease for short pulse separations in our device.

### 3. Thermal diffusion model

Following the described investigation we have developed a simplified model for the thermal diffusion after the discharge, in order to draw the dependence of the optical cavity recovery time on the various laser parameters. For simplicity we have calculated only the diffusion in the direction normal to the discharge plane ( $x$  direction), were we have observed the largest effect on the HeNe probe laser.

After the pressure relaxation, which takes place with the speed of sound across the discharge (after  $\approx 10 \mu\text{s}$ ), the medium perturbation can be described by the temperature function

$$T(x, t) = T_0 [1 + u(x, t)], \quad (1)$$

where  $T_0$  is the equilibrium temperature.

Neglecting convection phenomena, the perturbation function  $u(x, t)$  has to satisfy the Fourier equation

$$\chi \partial^2 u / \partial x^2 = \partial u / \partial t, \quad (2)$$

where  $\chi = \kappa / \rho c_p$  ( $\kappa$  = thermal conductivity,  $\rho$  = gas density,  $c_p$  = constant pressure specific heat) [17].

Assuming for calculation simplicity a gaussian initial temperature distribution

$$u(x, 0) = (S/\sqrt{2\pi}\Delta) \exp(-x^2/2\Delta^2) \quad (3)$$

where  $\Delta$  is a measure of the discharge width and  $S$  is a normalization coefficient related to the energy deposited in the discharge, and neglecting the variation of  $\chi$  with density during the diffusion, the solution of (2) with boundary condition at infinity is

$$u(x, t) = \frac{u(0, 0)}{(1 + t/t_0)^{1/2}} \exp\left(-\frac{x^2}{2\Delta^2(1 + t/t_0)}\right) \quad (4)$$

with  $t_0 = \Delta^2/2\chi$ .

The presence of the walls at a distance  $d$  from the discharge plane will not affect this solution until  $u(d, t)$  is small. Since  $d$  is much larger than the discharge width, the walls can only modify the tail of the diffusion.

From (4) we see that, even though  $t_0$  can be assumed as a measure of the thermal recovery time, one has to wait many times  $t_0$  to have a substantial reduction of the perturbation. Since  $\kappa = 2D\rho c_v$  ( $D$  = diffusion coefficient,  $c_v$  = constant volume specific heat) [18] we can write

$$\chi = 2Dc_v/c_p$$

and assuming  $D = 0.8 \text{ cm}^2 \text{ s}^{-1}$  [18] and  $\Delta = 0.25 \text{ cm}$  we obtain  $t_0 \approx 30 \text{ ms}$ .

Using the ideal gas equation

$$\rho(x, t) = \rho_0/[1 + u(x, t)], \quad (5)$$

where  $\rho_0$  is the equilibrium gas density, and the empirical Gladstone–Dale equation

$$n(x, t) = 1 + C\rho(x, t), \quad (6)$$

the perturbation function can be related to the refractive index of the medium [19].

From (4) and (5) we find for the temporal evolution of the density on the laser axis

$$\rho(0, t) = \frac{\rho_0}{1 + u(0, 0)/(1 + t/t_0)^{1/2}} \quad (7)$$

The optical path for paraxial rays in the perturbed medium can easily be found developing the density function to the second order in  $x$

$$\rho(x, t) = \rho(0, t) + [\beta^2(t)/2C]x^2 \quad (8)$$

and solving the ray equation

$$(d/ds)(n dr/ds) = \nabla n. \quad (9)$$

A paraxial ray impinging on the medium parallel to the laser axis at a distance  $x_0$  from the discharge plane will be deflected, at the end of the laser, up to  $x_f$  given by

$$x_f = x_0 \cosh(\beta l) \quad (10)$$

where  $l$  is the discharge length [20].

Therefore the intensity of the discharge induced optical perturbation and its time evolution can be evaluated from the expression

$$\beta^2(t) = \frac{C\rho_0}{\Delta^2} \frac{u(0, t)}{[1 + u(0, t)]^2} \frac{1}{(1 + t/t_0)}, \quad (11)$$

showing the possibility of improving the PRR capability of a discharge RGH laser with static fill either reducing the perturbation intensity, related to  $\beta^2(0)$ , or the recovery time  $t_0$ .

However a reduction of  $t_0$  with an effective cooling of the gas between pulses at high PRR would require a substantial reduction of discharge width, which

would be better pursued in a confined discharge geometry, taking advantage of the heat transfer at the walls. On the contrary, the transmission properties of the medium after the discharge can be favourably affected by an increase of the discharge width, reducing, for a given energy deposition density, the intensity of the optical perturbation.

#### 4. High PRR optimization study

Fig. 4 presents curves of normalized lasing energy with double pulse excitation ( $E_2/E_1$ ) as a function of delay  $T$  for various laser configurations. Comparison of these data with fig. 2 shows that by suitably selecting the operating point (pumping energy, gas mixture composition, filling pressure) it was possible to obtain a remarkable decrease of the laser recovery time  $\tau$ , defined as the pulse delay which reduces to a half the second pulse laser output ( $E_2/E_1 = 0.5$ ).

Since the thermal recovery time  $t_0$  does not change significantly between the different configurations, the observed reduction in laser recovery time  $\tau$  can be ascribed to a reduction of the perturbation intensity, as it was also shown by the HeNe transmission experiments.

The experimental results can be qualitatively explained by taking into account the described analysis of thermal effects and assuming, accordingly with the

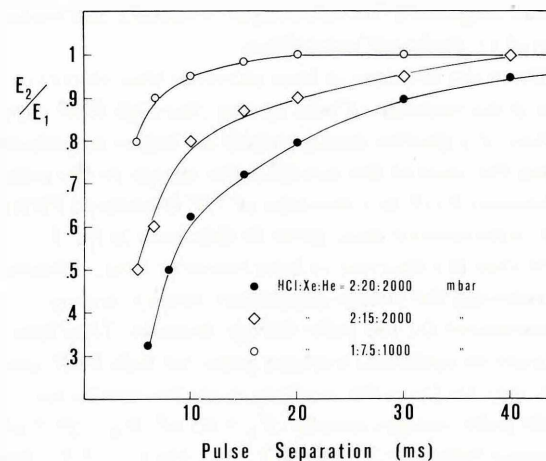


Fig. 4. Normalized energy of the second laser pulse versus pulse separation in the configuration  $C_1 = 45 \text{ nF}$ ,  $C_2 = 22.5 \text{ nF}$ ,  $HV = 25 \text{ kV}$ .

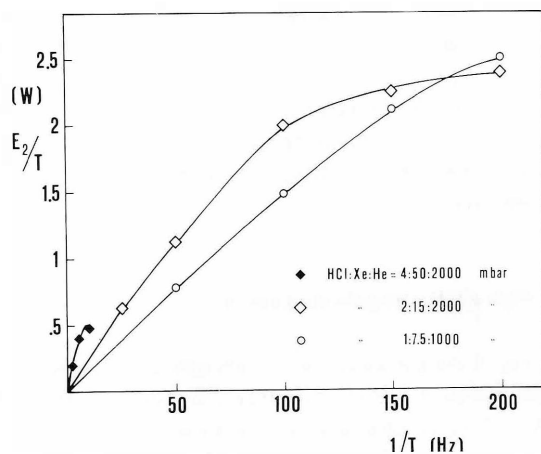


Fig. 5. Ratio of the second laser pulse energy to the pulse separation  $E_2/T$  versus simulated PRR ( $1/T$ ) for various laser configurations: ◆)  $C_1 = 80$  nF,  $C_2 = 50$  nF, HV = 30 kV; ◇), ○)  $C_1 = 45$  nF,  $C_2 = 22.5$  nF, HV = 25 kV.

experimental observations, that a lower concentration of Xe and HCl, besides decreasing the breakdown voltage, favours a wider discharge. The slow energy decrease for delays from 40 ms to 10 ms is in agreement with the slow variation of  $\beta(t)$  and  $\rho(t)$  in this delay range.

Current pulse and breakdown voltage measurements did not show any noticeable difference for delays as short as 5 ms.

The fluorescence always showed an increase in amplitude fluctuations in the region of abrupt laser decrease, suggesting the occurrence of density fluctuations related to discharge instabilities.

Since the decrease in laser recovery time always occurs at the expense of laser energy, the high PRR capabilities of a specific configuration are better summarized giving the ratio of the second pulse energy to the pulse separation  $E_2/T$  as a function of  $1/T$  (simulated PRR). The experimental data, given in this form in fig. 5, show that the decrease in laser recovery time, obtained by reducing the energy deposition density, widely compensates for the pulse energy decrease. They also indicate an optimum working point for high PRR operation very far from the working point for maximum single pulse energy, namely:  $C_1 = 45$  nF,  $C_2 = 22.5$  nF, charging voltage = 25 kV, HCl : Xe : He = 1 : 7.5 : 1000 mbar. In this situation an energy of 12.5 mJ from the second pulse with a ratio  $E_2/E_1 \approx 0.8$  has been measured for  $T = 5$  ms.

## 5. Conclusions

We have carried out an experimental investigation of the effects limiting the high PRR operation of discharge pumped XeCl lasers without gas circulation. The potential high PRR capabilities of the laser were assessed by double pulse experiments. The major limitation on the PRR in a laser optimized for the single pulse energy was found to be the thermal perturbation of the active medium. By suitably selecting the laser parameters (energy deposition, gas mixture composition, filling pressure), following a simplified analysis of the thermal effects, we have been able to reduce the perturbation intensity to a level which allows lasing from the second pulse with an energy of 12.5 mJ for delays as short as 5 ms.

In this laser configuration the main cause of energy decrease for short pulse delays was supposed to be a local density fluctuation related to discharge instabilities.

The above results can be useful as guidelines for the average power optimization of static fill lasers. Moreover we believe that they can also be useful for the optimization of gas flowing laser systems, allowing a reduction in the number of discharge volume clearances required between pulses for a given output power.

## References

- [1] T.S. Fahlen, J. Appl. Phys. 49 (1978) 455.
- [2] C.P. Wang, Appl. Phys. Lett. 32 (1978) 360.
- [3] C.P. Wang and O.L. Gibb, IEEE J. Quantum Electron. QE-15 (1979) 318.
- [4] J.L. Miller, J. Dickie, J. Davin, J. Swingle and T. Kan, Appl. Phys. Lett. 35 (1979) 912.
- [5] V.Y. Baranov, G.S. Baronov, V.M. Borisov, Y.B. Kiryukhin and S.G. Mamonov, Sov. J. Quantum Electron. 10 (1980) 512.
- [6] T.S. Fahlen, IEEE J. Quantum Electron. QE-16 (1980) 1260.
- [7] P.E. Cassady, G. Mullaney and S.R. Byron, CLEO '81, Washington DC, June, 1981.
- [8] R.C. Sze and E. Seegmiller, IEEE J. Quantum Electron. QE-17 (1981) 81.
- [9] D.P. Christensen, Appl. Phys. Lett. 30 (1977) 483.
- [10] V.N. Ishchenko, V.N. Lisitsyn and A.M. Razhev, Sov. Techn. Phys. Lett. 3 (1977) 281.
- [11] J.L. Newmann, Appl. Phys. Lett. 33 (1978) 501.
- [12] A.J. Mendelsohn, R. Normandin, S.E. Harris and J.F. Young, CLEO '81, Washington DC, June, 1981.

- [13] Kan-Ich Fujii, A.G. Kearsley, A.J. Andrews, K.H. Errey and C.E. Webb, IEEE J. Quantum Electron. QE-17 (1981) 1315.
- [14] C.A. Brau, Rare gas halogen excimers, in: Excimer lasers, ed. C.K. Rhodes (Springer Verlag, Berlin, 1979) p. 98, 105.
- [15] R.W. Waynant and J.G. Eden, Appl. Phys. Lett. 36 (1980) 262.
- [16] R.C. Sze and T.R. Loree, J. Quantum Electron QE-14 (1978) 944.
- [17] L. Landau and E. Lifchitz, Mécanique des fluides (MIR, Moscou, 1971).
- [18] S. Chapman and T.G. Cowling, The mathematical theory of non uniform gases (Cambridge University Press, London, 1970).
- [19] M.C. Gower, Optics Comm. 12 (1974) 244.
- [20] R. Buffa, Ph.D. thesis, University of Florence, Italy, 1980, unpublished.